Proceedings of the ASME 2014 Conference on Smart Materials, Adaptive Structures and Intelligent Systems
SMASIS2014
September 8-10, 2014, Newport, Rhode Island, USA

SMASIS2014-7686

EXPERIMENTAL INVESTIGATIONS ON VISCOELASTIC PROPERTIES OF A SHAPE MEMORY POLYMER

Pauline Butaud
FEMTO-ST Applied Mechanics
University of Franche-Comté
Besançon, France
Email: pauline.butaud@femto-st.fr

Morvan Ouisse
Vincent Placet
Emmanuel Foltête
FEMTO-ST Applied Mechanics
Besançon, France

ABSTRACT

The shape memory polymers (SMPs) are polymeric smart materials which have the remarkable ability to recover their primary shape from a temporary one under an external stimulus. The study deals with the synthesis and the thermo-mechanical characterization of a thermally-actuated SMP, the tBA/PEGDMA, with a special focus on viscoelastic properties. The mechanical characterization is performed using three kinds of tests: quasi-static tensile tests, dynamic mechanical analysis (DMA) and modal tests. The first one allows the identification of the Youngs modulus and the Poisson's ratio at ambient temperature. Modal analyses are done for various temperature values, and resonance frequencies are measured. In order to validate the time-temperature equivalence on this SMP, a DMA is performed under harmonic loading for different temperatures and a master curve highlights a complementarity of the results. Finally a suitable model for the viscoelastic behavior of the SMP is identified.

INTRODUCTION

Shape memory polymers (SMPs) belong to the class of smart materials. These materials have found growing interest throughout the last few years. Indeed, in some aspects, SMPs are more efficient than the well-known metallic shape memory alloy (SMAs). SMPs particularly offer recoverable strain that can reach 400% (to be compared to 8% for SMAs), light weight, easy manufacturing and cheapness compared to SMA [1]. They can be used in a large variety of applications, e.g. actuators, electromechanical systems, clothing manufacturing, morphing and deployable space applications, control of structures, self-healing, biomedical devices and so on [2] [3]. The SMPs have the ability of changing their shape in response to an external stimulus [4], most typically thermal activation. When the SMP is heated above the glass transition temperature T_g, it is soft and rubbery and it is easy to change its shape. If the SMP is subsequently cooled below T_g, it retains the given shape (shape fixing characteristic). When heated again above T_g, the material autonomously returns to its original permanent shape [5]. The shape-memory effect is in principle a behavior inherent to all polymers. However, polymers that exhibit truly exploitable shape-memory effect must demonstrate a sharp transition temperature and a rubbery plateau, along with relatively large strain capacity without local material damage [6]. The memory effect of SMP is quite depending on the level of external constraint. For example if the stiffness of the constraining material is equal to the stiffness of the shape memory polymer in the rubbery state, the polymer will only recover half of its total strain [7].

The increasing use of SMP for quasi-static and dynamic applications, under various temperature ranges, has made necessary the characterization of these materials over wide frequency bands [8]. Three kinds of tests have been performed in this study. First, quasi-static tensile test are used at ambient temperature and at a controlled loading rate allowing identification of the apparent Young's modulus. Then, a dynamic mechanical analysis (DMA) is used to determine the evolution of viscoelastic properties as

a function of the temperature and loading frequency. Finally, a modal analysis has been performed to reach higher loading frequencies. In this last technique, a finite element model is employed to identify the viscoelastic properties of the material from the dynamic measurements. The main purpose of this work is to check the validity of the time-temperature equivalence [9] obtained from the DMA measurements, use this equivalence to find the master curves of the material, and finally identify a suitable model for the viscoelastic behavior of the SMP.

MATERIALS AND EXPERIMENTAL METHODS

Material and specimen preparation

As a representative thermally-actuated shape-memory polymer, a chemically-crosslinked thermoset polymer recently studied by Yakacki et al. [10] and Srivastava et al. [11] is chosen. Following the procedure described by these authors, the SMP is synthesized by manually mixing 95 wt% of the monomer tert-butyl acrylate (tBA) with 5 wt% of the crosslinking agent poly(ethylene glycol) dimethacrylate (PEGDMA) (with typical molecular weight $M_n = 550$ g/mol). The photoinitiator, 2,2-dimethoxy-2-phenylacetophenone (DMPA), is added to the solution at a concentration of 0.5 wt% of the total weight. The liquid mixture is then injected between two glass slides separated by a 3 mm spacer. The polymerization is initiated by exposing the solution to UV light during 10 minutes and achieved by heating the polymer at 90 ° C for 1 hour. One of the obtained plates, measuring 200×150 mm, was machined with a CNC machine. Dog-bone shaped specimens were produced from the polymer plate for quasi-static tensile tests. The gauge length is 30 mm, and the rectangular cross section is 3×2.97 mm. In the same plate, samples for DMA testing were cut. Their dimensions are $29 \times 6 \times 2.97$ mm. Another plate was produced with the same protocol for the modal analysis measurements.

Mechanicals tests

Quasi-static tests The quasi-static tensile test have been performed using a universal commercial testing machine (Instron 6025) with a capacity of $\pm$ 100 kN. The specimen, clamped using wedge action grips, was subjected to a displacement control feedback at 0.1 mm/s ie a strain rate of $4.10^{-}3$ Hz. The test was performed at ambient temperature 22 ° C ($\pm$ 1 ° C). The engineering longitudinal strain was measured by a laser extensometer (EIR LE05) with a displacement accuracy of approximately 1 μm. The gauge part of the specimen for the strain measurement is 30 mm in length. The longitudinal Young's modulus was determined by the slope of the stress-strain curve at 0.01% of engineering strain (tangent modulus technique).

Dynamic mechanical analysis The frequency and temperature dependence of the viscoelastic material's properties can be described by a complex modulus $E^*(\omega)$:

$$E^*(\omega) = E'(\omega) + iE''(\omega) = E'(\omega)(1 + i\tan(\delta)). \quad (1)$$

Viscoelastic properties (storage modulus E', loss modulus E'' and loss factor $\tan(\delta)$) are measured using a METRAVIB DMA50 apparatus every 5 ° C or 10 ° C in isothermal conditions. Temperature varies between 0 ° C and 90 ° C and the frequency of the excitation from 0.1 Hz to 180 Hz according to the temperature. A sinusoidal tensile displacement was applied on the sample with a peak-to-peak amplitude of 10^{-4} m, in order to test the specimen in the linear viscoelastic range.

Modal analysis The studied structure is a tBA/PEGDMA rectangular plate with the following dimensions $157.7 \times 45.5 \times 3.1$ mm ($\pm$ 0.1 mm). The plate is suspended in order to assess free-free conditions. Contactless actuators and sensors are used. The external force is applied thanks to a voice-coil actuator with a permanent magnet glued in a corner of the plate. This assembly is placed in a thermal chamber with a temperature control between 22 and 36 ° C every 7 ° C ($\pm$ 2 ° C). A broadband random excitation is applied between 150 and 4000 Hz. The plate response is measured by using a laser vibrometer (Polytec OFV-505) successively focused on 28 reflecting stickers spread on the plate. The modal frequencies, the modal damping and the mode shapes are then identified by using Modan^{TM} (modal analysis software) on the frequency response functions (FRFs). At the same time, a finite element model is established on Patran^{TM}2012 under the hypothesis that the material is homogeneous and isotropic, with a Poisson's ratio $\nu = 0.37$ (determined from quasi-static tests), a mass density $\rho = 1004$ kg/m^3 (determined by measuring the plate's mass and volume) and a presumed Young's modulus $E = 2000$ MPa. The magnet is included in the numerical model ($E = 210\,000$ MPa, $\nu = 0.33$, $\rho = 7460$ kg/m^3). Finally a model-test correlation is performed on AESOP^{TM} software and a model updating procedure is conducted to obtain the mechanical parameters of the tBA/PEGDMA at the modal frequencies.

Kinematic fields measurement An optical camera (Ueye 1Mpixel 8bit) was used during the quasi-static test to assess the displacements fields in the gauge part of the specimen using digital image correlation (DIC). The camera was equipped of a telecentric lens (0.20x Techspec Silver series telecentric lens - 63073 - Edmund Optics) that prevents measurements from optical distortions. It also ensures a large depth of field (of approximately 6 mm) which guarantees the sharpness of images even in case of necking. Image acquisition was triggered with a Labview application at a frequency of 1 frame per sec. DIC was performed

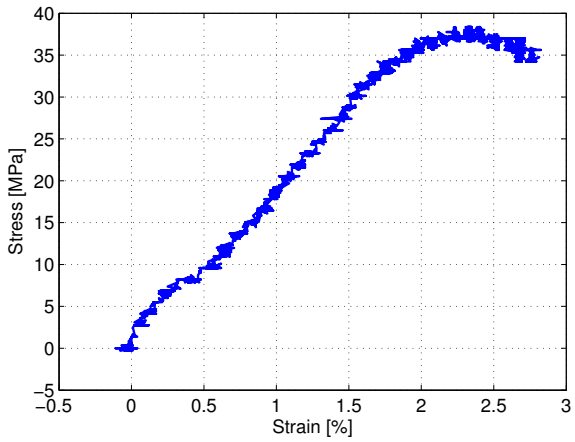

FIGURE 1. Stress-strain curves obtained from a tensile test at a speed of 4×10^{-3} s^{-1}, for tBA/PEGDMA, at ambient temperature 22 ° C.

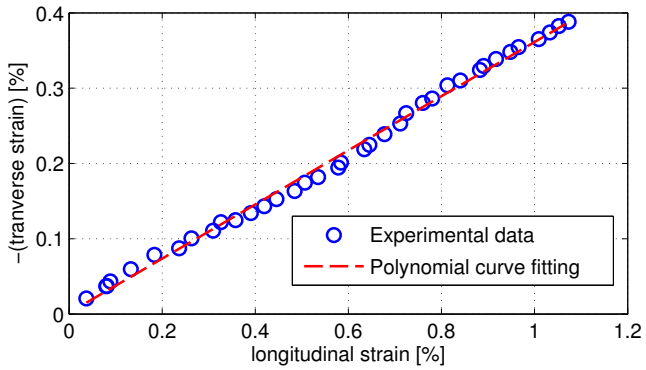

FIGURE 2. Identification of the Poisson's ratio, by polynomial curve fitting, around 0.37 at 4×10^{-3} s^{-1}, for tBA/PEGDMA, at 22 ° C.

with a free home-made global correlation code, implemented in Octave and described by Maynadier et al. [12]. Quadratic elements were chosen for meshing the area of interest. The strain fields were computed from the displacement fields by pixel-wise difference gradient.

RESULTS

Quasi-static characterization

Fig. 1 shows the stress-strain curve obtained from the quasi-static test. The apparent Young's modulus is approximately 1900 MPa, the ultimate stress (38 MPa) is reached at a strain of 2.3 % and the elongation at rupture is about 2.8 % for a strain rate of 4×10^{-3} s^{-1}.

The Poisson's ratio was determined using the strain fields determined using DIC. The value is approximately 0.37 (Fig. 2).

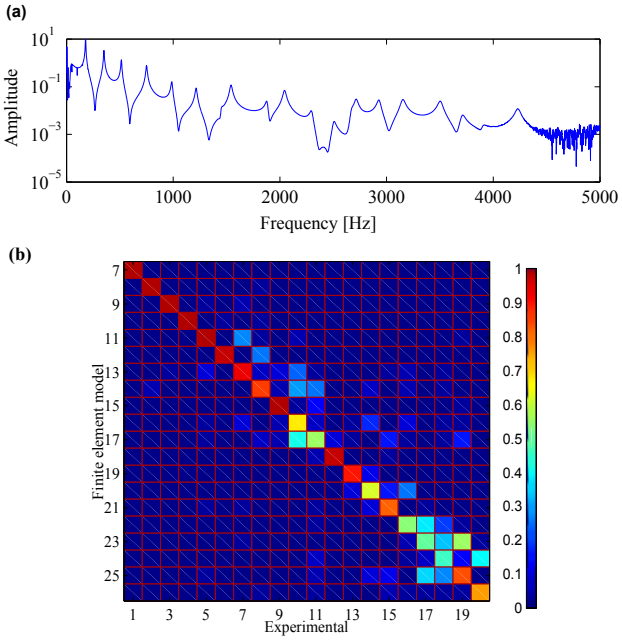

FIGURE 3. (a) FRFs and (b) MAC Matrix for 22 ° C experimental data.

Modal analysis

Modal vibration tests allow identification of the eigen modes of the shape memory plate. A MAC (modal assurance criteria) value over 0.7 is used as a matching criterion for these modes. Depending on the temperature, 11 to 13 modes are paired with modes issued from the finite element model after the model-test correlation (Fig. 3).

After the model updating procedure, the Young's modulus and tan(δ) of the tBA/PEGDMA are determined. Their evolution with temperature and frequency are shown in Fig. 4.

The storage modulus decreases as expected with increasing temperature, but its variation with the frequency is unusual, as it seems to decrease also. This trend is not well understood yet, even if some hypotheses are considered. For example, the Poisson's ratio used in the finite element model was determined in quasi-static regime whereas it could fluctuate with the frequency like the storage modulus. Other hypotheses like the isotropic character of the material are currently under investigation.

Dynamic mechanical analysis

The results of the DMA tests are shown in Fig. 5. The storage modulus E' decreases with the temperature and increases with the frequency. These trend is consistent with the behavior of a classical polymer. Moreover the values of E' and loss factor tan(δ) at 1 Hz are consistent with the results obtained by Ortega

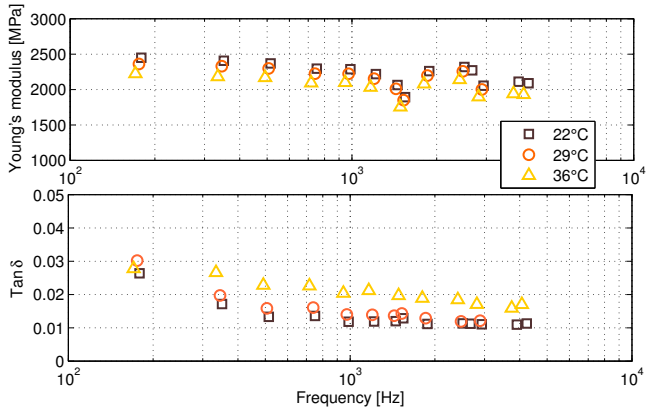

FIGURE 4. Storage modulus E' and loss factor tan(δ) determined by modal analysis according to the frequency and for several temperatures.

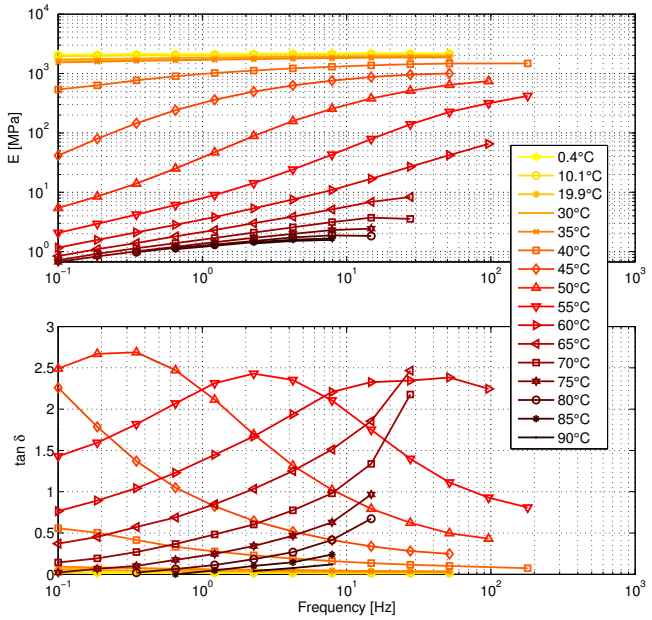

FIGURE 5. Storage modulus E' and loss factor tan(δ) measured by DMA according to the frequency f and for several temperatures.

et al. [13] for the same material. The large gap between the glass state modulus and the rubbery modulus (the ratio exceeds 3000), is a specificity of shape memory polymers. The glass transition temperature T_g is located between 45 ° C and 55 ° C. In this range of temperature, the viscoelastic properties of the tBA/PEGDMA are really interesting, indeed the value of the loss factor is higher than 1.5 in a wide range of frequencies and can reach a maximal value of 2.5 .

According to the Cole-Cole plot, where all data lie close

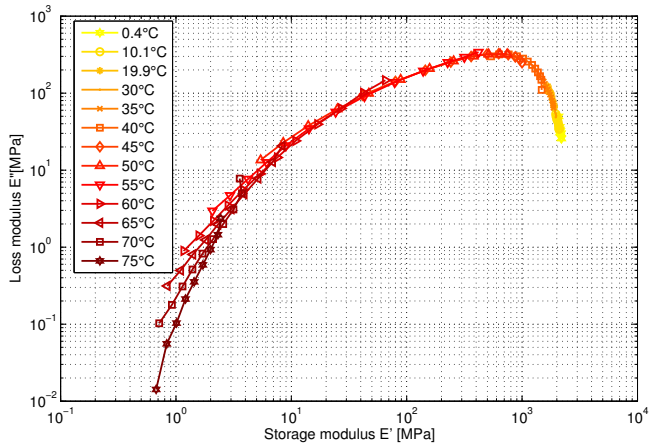

FIGURE 6. Cole-Cole plot of the complex modulus of the tBA/PEGDMA.

to a single curve (Fig. 6), it is possible to conclude that the tBA/PEGDMA is thermo-rheological simple [14]. Thus curves of E' and tan(δ) vs. frequency (Fig. 5) at one temperature can be shifted horizontally to overlap with adjacent curves without vertical shifting because of the thermo-rheological simplicity. The time-temperature superposition shift factors a_T used for E' must be the same for tan(δ) to get time-temperature equivalence [15]. In our case, the shift factors a_T are obtained through an optimization procedure (classical least square method) for a reference temperature T_0 selected arbitrarily and are equivalent for both E' and tan(δ), therefore the time-temperature equivalence is validated in the considered temperature and frequency ranges for the tBA/PEGDMA. The master curves of the storage modulus and loss factor are given in Fig. 7.

In this work,the temperature evolution of the shift factor a_T is expressed according to Williams- Landel-Ferry [16] (or WLF) equation by

$$\log a_T = \frac{-C_1^0 (T - T_0)}{C_2^0 + (T - T_0)}, \tag{2}$$

which can also written as

$$\frac{T - T_0}{\log a_T} = -\frac{1}{C_1^0}(T - T_0) - \frac{C_2^0}{C_1^0}, \tag{3}$$

with $C_1^0 = 10.87$ and $C_2^0 = 32.57$ ° C for a reference temperature T_0 of 40 ° C (Fig. 8).

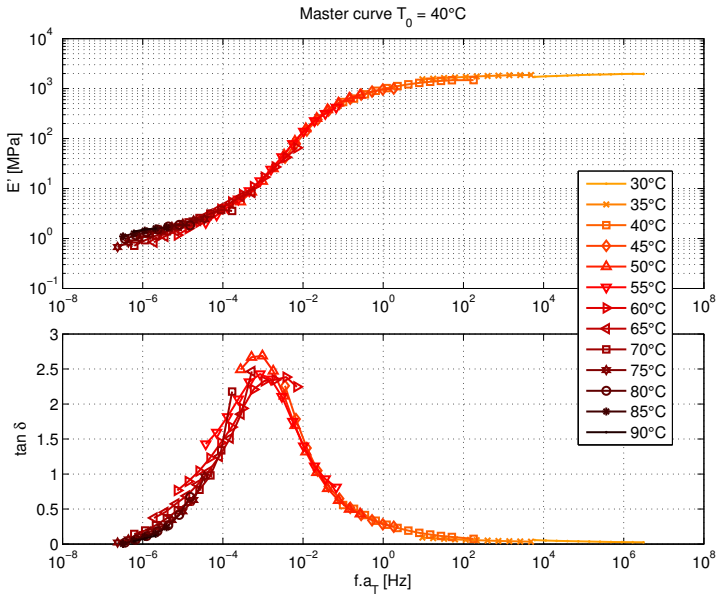

FIGURE 7. Master curves of E' and $\tan(\delta)$ according to the reduced frequency $f.a_T$ with a reference temperature of 40 ° C.

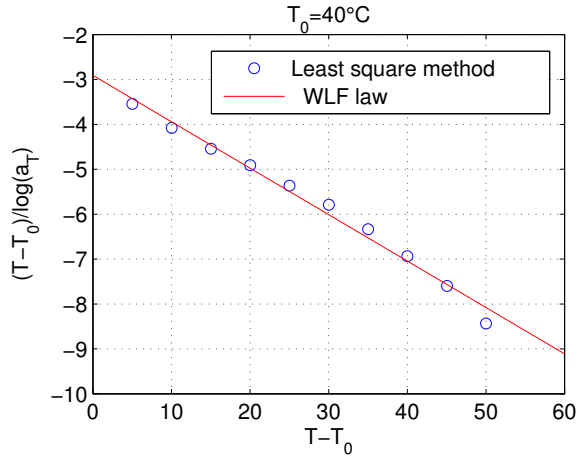

FIGURE 8. a_T : experimental data from dynamic analysis and WLF equation

MODELING OF VISCOELASTIC BEHAVIOR

Fractional derivative Zener model

The Zener model [17] provides the expression of the elastic complex modulus as

$$E^*(\omega) = \frac{E_0 + E_\infty (i\omega\tau)^\alpha}{1 + (i\omega\tau)^\alpha}. \qquad (4)$$

TABLE 1. Zener model parameters for the SMP tBA/PEGDMA.

E_0 (MPa)	E_∞ (MPa)	α	τ_0 (s)
0.67	2211	0.78	0.91

Its behavior in the frequency domain is described between two asymptotic values, namely the static elastic modulus E_0 and the high-frequency limit value of the dynamic modulus E_∞ ; τ is the relaxation time and α is the order of the fractional derivative. The statements $0 < \alpha < 1$, $\tau > 0$ and $E_\infty > E_0$ must hold to fulfill the second law of thermodynamics. An estimation of the four parameters E_0, E_∞, α and τ from experimental measurements is given in [18]:

$$\begin{cases} E_0 = \lim\limits_{\omega\to 0} E^*(\omega), \\ E_\infty = \lim\limits_{\omega\to\infty} E^*(\omega), \\ \alpha = \dfrac{2}{\pi}\arcsin\left[\tan(\delta_{\text{pic}})(E_\infty - E_0) \right. \\ \qquad \left. \times \dfrac{2\sqrt{E_0 E_\infty} + (E_\infty + E_0)\sqrt{1+\tan^2(\delta_{\text{pic}})}}{\tan^2(\delta_{\text{pic}})(E_\infty + E_0)^2 + (E_\infty - E_0)^2}\right], \\ \tau = \dfrac{1}{\omega_{\text{pic}}}\left(\dfrac{E_0}{E_\infty}\right)^{\dfrac{1}{2\alpha}}, \end{cases} \qquad (5)$$

where ω_{pic} is the frequency corresponding to the maximum of the loss factor $\tan(\delta_{\text{pic}})$. The parameters of the fractional derivative Zener model obtained for the tBA/PEGDMA are given in Tab. 1.

The Fig. 9 compares the master curves of the dynamical properties (storage modulus and loss factor) obtained from experimental measurements with the ones coming from the Zener model, given by Eqn. (4). The viscoelastic behavior of the tBA/PEGDMA, predicted by the Zener model with only four parameters, seems reliable. Moreover, the identification of the 4 parameters is obvious. However, a close look at the transition region indicates that the Zener model is not able to represent the asymmetry of the $\tan(\delta)$ peak. This is the reason why a more general model is used in the next section.

2S2P1D model

The 2S2P1D model, whose name comes the abbreviation of the combination of two springs, two parabolic creep element and one dashpot [19], is a model allowing description of the rheological properties of a viscoelastic material with an asymmetric loss factor. For a given temperature, the 2S2P1D model is based on seven parameters, all with a physical meanings, to estimate the

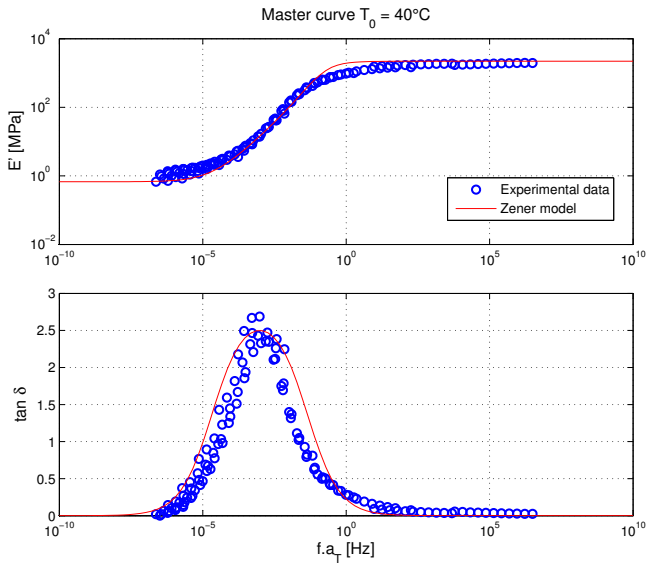

FIGURE 9. Master curves of tBA/PEGDMA for T_0 =40 ° C compared with the Zener model.

value of the complex modulus as

$$E^*(i\omega\tau) = E_0 + \frac{E_0 - E_\infty}{1+\gamma(i\omega\tau)^{-k}+(i\omega\tau)^{-h}+(i\omega\beta\tau)^{-1}}, \quad (6)$$

where k and h are exponents with $0 < k < h < 1$, γ and β are constants, E_0 is the rubber modulus when $\omega \to 0$, E_∞ is the glassy modulus when $\omega \to \infty$ and τ is the characteristic time, a function of temperature. τ evolution might be approximated by the WLF equations

$$\tau(T) = a_T(T).\tau_0, \quad (7)$$

where $a_T(T)$ is the shift factor at the temperature T and $\tau_0 = \tau(T_0)$ is determined at the reference temperature T_0. In this work we applied the 2S2P1D model to the tBA/PEGDMA. The parameters have been estimated using an optimization procedure based on least squares, directly from experimental data. For this SMP the parameters are given in Tab. 2.

As can be seen from Fig. 10 a good fit is obtained between the 2S2P1D and the experimental measurements, on a wide frequency band. Compared to the Zener model, this model requires more efforts for parameters identification, but the result is really consistent with the experimental tests.

Comparison with the experimental data

Thanks to the WLF law, it is therefore possible to investigate the coherence of the quasi static results, the modal analysis and the viscoelastic models (Zener and 2S2P1D), as shown on Fig. 11. The reference temperature which has been choosen is 22 ° C, according to the quasi-static test temperature.
The Young's modulus measured in quasi-static test is slightly lower than the value predicted by the viscoelastics models. However, it is quite difficult to define the frequency of the quasi-static test. Indeed, it is assumed here that the strain rate is equivalent to the frequency of the excitation which involves some uncertainties and so can explain the gap on the modulus value.
The complex modulus values, determined at 22 ° C between 200 Hz and 4000 Hz, by modal analysis, are consistent with the high-frequency limit value of the complex modulus identified in the two viscoelastics models. Concerning the data measured at 29 ° C and 36 ° C, the better correlation is obtained with the Zener model even though the 2S2P1D model was the most coherent for the DMA experimental results. However it should be remembered that the temperature control for this analysis was not enough precise ($\pm$ 2 ° C) and so can cause important gaps for these kind of comparison where the reduced frequency $f.a_T$ depends on the temperature.

TABLE 2. 2S2P1D model parameters for the SMP tBA/PEGDMA

E_0 (MPa)	E_∞ (MPa)	k	h	γ	β	τ_0 (s)
0.67	2211	0.16	0.79	1.68	3.8e+4	0.61

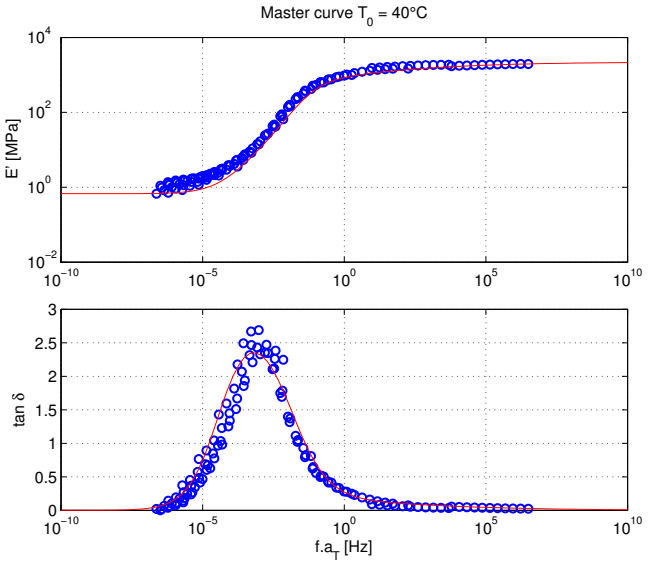

FIGURE 10. Master curves of tBA/PEGDMA at 40 ° C compared with the 2S2P1D model

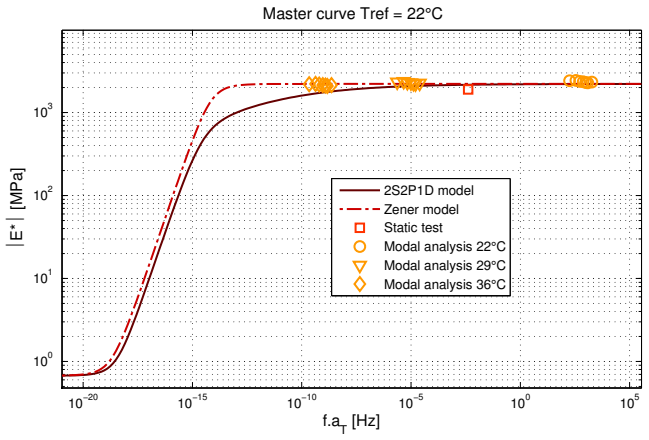

FIGURE 11. Complex modulus according to reduced frequency for models and experimental data.

Actually, for a greater understanding and to validate the viscoelastic models, a modal test during the glass transition would be welcome, but it is quite difficult in practice due to the very low stiffness of the tBA/PEGDMA around T_g.

CONCLUSION

The objective of this study was to highlight the time-temperature equivalence by comparing three experimental methods allowing the identification of the storage modulus over frequency and temperature. This equivalence has been checked on a sample tested with the DMA. Quasi-static tests and modal analysis have been carried out to explore a wider frequency band. Two viscoelastics models have been determined, thanks to the master curve and the WLF law associated, and reflect pretty well the viscoelastic properties of the tBA/PEGDMA on a wide band of frequency, even during the glass transition. Finally a comparison between these models and the experimental data has been done and shows a quite good coherence at high frequency, whereas low frequencies remain to be investigated.

ACKNOWLEDGMENT

The authors thank ACOEM/01dB-Metravib for the dynamic mechanical analysis of the tBA/PEGDMA.
This work was co-financed by The French National Research Agency under grant number ANR-12-JS09-008-COVIA. It has been performed in cooperation with the Labex ACTION program (ANR-11-LABX-0001-01).

REFERENCES

[1] Pretsch, T., 2010. "Review on the Functional Determinants and Durability of Shape Memory Polymers". *Polymers,* ***2***(3), July, pp. 120–158.

[2] Behl, M., and Lendlein, A., 2007. "Shape-memory polymers are an emerging class of active polymers that". pp. 20–28.

[3] Dietsch, B., and Tong, T., 2007. "A review-: Features and benefits of shape memory polymers (smps)". *Journal of advanced materials,* ***39***(2), pp. 3–12.

[4] Ratna, D., and Karger-Kocsis, J., 2008. "Recent advances in shape memory polymers and composites: a review". *Journal of Materials Science,* ***43***(1), pp. 254–269.

[5] Wilson, S. A., Jourdain, R. P., Zhang, Q., Dorey, R. A., Bowen, C. R., Willander, M., Wahab, Q. U., Willander, M., Nur, O., Quandt, E., Johansson, C., Pagounis, E., Wilson, S., and Bowen, C., 2007. "New materials for micro-scale sensors and actuators . An engineering review". pp. 1–129.

[6] Sillion, B., 2002. "Les polymères à mémoire de forme". pp. 182–188.

[7] Liu, Y., Gall, K., Dunn, M. L., Greenberg, A. R., and Diani, J., 2006. "Thermomechanics of shape memory polymers: Uniaxial experiments and constitutive modeling". *International Journal of Plasticity,* ***22***(2), Feb., pp. 279–313.

[8] Lendlein, A., and Kelch, S., 2002. "Shape-memory polymers". *Angewandte Chemie International Edition,* ***41***(12), pp. 2034–2057.

[9] Okubo, N., 1990. "Preparation of Master Curves by Dynamic Viscoelastic Measurements". *SII NanoTechnology Inc.,* ***6***.

[10] Yakacki, C. M., Shandas, R., Lanning, C., Rech, B., Eckstein, A., and Gall, K., 2007. "Unconstrained recovery characterization of shape-memory polymer networks for cardiovascular applications". *Biomaterials,* ***28***(14), pp. 2255 – 2263.

[11] Srivastava, V., Chester, S. a., and Anand, L., 2010. "Thermally actuated shape-memory polymers: Experiments, theory, and numerical simulations". *Journal of the Mechanics and Physics of Solids,* ***58***(8), Aug., pp. 1100–1124.

[12] Maynadier, a., Poncelet, M., Lavernhe-Taillard, K., and Roux, S., 2011. "One-shot Measurement of Thermal and Kinematic Fields: InfraRed Image Correlation (IRIC)". *Experimental Mechanics,* ***52***(3), Mar., pp. 241–255.

[13] Ortega, A. M., Kasprzak, S. E., Yakacki, C. M., Diani, J., Greenberg, A. R., and Gall, K., 2008. "Structure–property relationships in photopolymerizable polymer networks: Effect of composition on the crosslinked structure and resulting thermomechanical properties of a (meth) acrylate-based system". *Journal of applied polymer science,* ***110***(3), pp. 1559–1572.

[14] Rouleau, L., Deü, J.-F., Legay, a., and Le Lay, F., 2013. "Application of KramersKronig relations to timetempera-

ture superposition for viscoelastic materials". *Mechanics of Materials,* ***65***, Oct., pp. 66–75.

[15] Dealy, J., and Plazek, D., 2009. "Time-temperature superposition?a users guide". *Rheol. Bull,* ***78***(2), pp. 16–31.

[16] Williams, M. L., Landel, R. F., and Ferry, J. D., 1955. "The temperature dependence of relaxation mechanisms in amorphous polymers and other glass-forming liquids". *Journal of the American Chemical Society,* ***77***(14), pp. 3701–3707.

[17] Rouleau, L., Deü, J.-F., Legay, A., and Sigrist, J.-F., 2012. "Vibro-acoustic study of a viscoelastic sandwich ring immersed in water". *Journal of Sound and Vibration,* ***331***(3), pp. 522–539.

[18] Galucio, A., Deü, J.-F., and Ohayon, R., 2004. "Finite element formulation of viscoelastic sandwich beams using fractional derivative operators". *Computational Mechanics,* ***33***(4), pp. 282–291.

[19] Yusoff, N. I. M., Mounier, D., Marc-Stphane, G., Hainin, M. R., Airey, G. D., and Benedetto, H. D., 2013. "Modelling the rheological properties of bituminous binders using the 2s2p1d model". *Construction and Building Materials,* ***38***(0), pp. 395 – 406.